J Neurophysiol 129: 894–899, 2023.
First published March 15, 2023; doi:10.1152/jn.00066.2023

american physiological society

JNP JOURNAL OF NEUROPHYSIOLOGY

RAPID REPORT

Differential reduction of gray matter volume with age in 35 cortical areas in men (more) and women (less)

Peka Christova[1,2]* and Apostolos P. Georgopoulos[1,2]*

[1]*Department of Veterans Affairs Health Care System, The Neuroimaging Research Group, Brain Sciences Center, Minneapolis, Minnesota, United States and* [2]*Department of Neuroscience, University of Minnesota Medical School, Minneapolis, Minnesota, United States*

Abstract

It is known that brain volume decreases with age. Here, we assessed the rate of this decrease in gray matter volume of 35 cortical regions in a large sample of healthy participants (n = 712, age range 36–90 yr) of the Human Connectome Project-Aging. We evaluated the difference in this rate between men (n = 316) and women (n = 396) and found that the volumes of cortical areas decreased by an average of 5.25%/decade, with the highest rate of decrease observed in the rostral anterior cingulate cortex (7.28%/decade). The rate of decrease was higher in men than in women in general and in 30/35 (85.7%) areas in particular, involving most prominently the cingulate lobe. These findings could serve as a normative reference for clinical conditions that manifest with abnormal brain atrophy.

NEW & NOTEWORTHY This study showed an overall decrease of cortical gray matter with age but with different rates of volume reduction in different areas, with smaller decrease rates in women than in men. The highest volume reduction rate was observed for the rostral anterior cingulate cortex, an area linked to depression. These findings could serve as a normative reference for clinical conditions that manifest with abnormal brain atrophy.

aging; cortex; Human Connectome Project-Aging; rostral anterior cingulate; sex

INTRODUCTION

Decreases in the volume of brain gray matter with increasing age have been reported consistently (1–4), albeit with variability among cortical (5) and subcortical regions (3, 6–8). In general, diverse methods have been used for such studies, including different acquisition parameters [different manufacturers, magnetic field strengths, magnetic resonance imaging (MRI) scanning protocols, etc.], methods for measuring gray matter volumes and parcellating regions, and atlases for labeling brain regions. Other aspects of such studies have varied widely as well, including the age range of the participants, the sample size (usually small), and the selection of specific areas (e.g., hippocampus). Here, we used MRI data of the Human Connectome Project in Aging (HCP-A) (9) to analyze the association between age and 35 cortical areas in a large sample of 712 healthy participants (316 men and 396 women) covering a wide range in adulthood in both sexes (36–90 yr old). A major, positive aspect of this data set is that data were acquired using the same state-of-the-art data collection method for all participants, including the hardware (3 T Siemens Prisma magnet), MRI image acquisition protocol, and MRI data processing (HCP structural pipelines). In summary, given the large sample size, wide age range, inclusion of both sexes, and state-of-the-art uniform acquisition methods, this data set was ideally suited to this study.

MATERIALS AND METHODS

Participants

Originally, data were acquired from 725 healthy participants (319 men and 406 women, age range 36–100 yr) (Human Connectome Project on Aging, www.humanconnectome.org/study/hcp-lifespan-aging) (9). However, ages for participants older than 90 yr were not provided, hence in this study we analyzed data from 712 participants (316 men and 396 women, 36–90 yr old). Exclusion criteria included clinical diagnoses of psychiatric and neurological disorders. All participants passed the Cognitive Status modified test and the Montreal Cognitive Assessment test (9).

*P. Christova and A. P. Georgopoulos contributed equally to the work.
Correspondence: P. Christova (savay001@umn.edu).
Submitted 9 February 2023 / Revised 6 March 2023 / Accepted 15 March 2023

0022-3077/23 Published by the American Physiological Society.

MRI Data Acquisition

A Siemens 3 T Prisma whole body scanner with 80 mT/m gradient coil was used (10). The 32-channel head coil enables high acceleration factors via multi-slice acquisitions. This advanced scanning technology allows whole brain imaging with submillimeter resolution of structural MRI. Acquired structural images are T1 weighted (T1w) multi-echo MPRAGE with duration of 8 min 22 s and T2 weighted (T2w) SPACE with duration of 6 min 35 s with volumetric navigator for prospective motion correction. Both structural scans use a sagittal field of view of 256 × 240 × 166 mm and 0.8 mm isotropic voxels. Other parameters of acquisitions are: for T1w scan—TE = 1.8/3.6/5.4/7.2 ms multi-echo, TR/TI = 2,500/1,000, flip angle = 8°, and for T2w scan—TR/TE = 3,200/564 ms, turbo factor = 314 (Ref. 10, p. 976).

MRI Data

Data were processed by three HCP structural pipelines: PreFreeSurfer Pipeline, FreeSurfer Pipeline, and PostFreeSurfer Pipeline with the aim of providing high-quality volume and surface data using the high-resolution T1w and T2w images. The pipeline is based on FreeSurfer version 6.0 software modified to capitalize on HCP's high-resolution data (11). Briefly, the surface-based FreeSurfer [FS; http://surfer.nmr.mgh.harvard.edu (12)] analysis involves normalization of image intensities and removal of extra-cerebral tissues, followed by segmenting the brain into gray and white matters and cerebrospinal fluid (CSF). Next, the boundaries between white matter, gray matter, pial surface, and CSF were estimated and registration was computed based on aligning the cortical folding patterns. The Desikan–Killiany atlas (13) parcellation scheme labels cortical sulci and gyri. We extracted the volumes of the following 35 areas × 2 hemispheres = 70 cortical areas in total (in alphabetical order): banks of superior temporal sulcus, caudal anterior cingulate cortex, caudal middle frontal gyrus, cuneus, entorhinal, frontal pole, fusiform, hippocampus, inferior frontal pars opercularis, inferior frontal pars orbitalis, inferior frontal pars triangularis, inferior parietal, inferior temporal, insula, isthmus cingulate, lateral occipital, lateral orbital frontal, lingual, medial orbital frontal, middle temporal, paracentral, parahippocampal, pericalcarine, postcentral, posterior cingulate, precentral, precuneus, rostral anterior cingulate, rostral middle frontal, superior frontal, superior parietal, superior temporal, supramarginal, temporal pole, transverse temporal cortex. The volumes of left and right hemisphere areas were averaged and analyzed as follows.

Statistical Analyses

Standard statistical methods (14) were used to analyze the data, linear regression, partial correlation, paired t test, and the Wilson test for testing single proportions (15). The statistical significance of the dependence of volume on age was determined by computing the partial correlation between volume and years, controlling for estimated total intracranial volume (eTIV). The percent change of volume with age was estimated by regressing the volume (adjusted for eTIV) against the years, and computing the ratio of the regression coefficient for years over the intercept:

$$\text{Volume adjusted for eTIV} = b_0 + b(\text{years}) + \text{error} \quad (1)$$

$$\text{Percent change of volume/year} = \text{PC/year} = 100\,\frac{b(\text{years})}{b_0} \quad (2)$$

and

$$\text{Percent change of volume/decade} = \text{PC/decade} = 10 \times \text{PC/year} \quad (3)$$

Data analyses were performed using MATLAB (version R2016) and the IBM-SPSS statistical package (version 27). All P values reported are two-sided.

RESULTS

Age

The age did not differ significantly between the two sexes with respect to its distribution (P = 0.314, Kolmogorov–Smirnov test), mean (P = 0.710, independent samples t test), and median (P = 0.291, independent samples median test). The mean age ± SD was 60.3 ± 15.2 yr for men (n = 316) and 59.1 ± 14.7 yr for women (n = 396); the medians were 59.0 and 57.0 yr for men and women, respectively.

Effect of Age on Volume

The volumes of all areas decreased highly significantly with age ($P < 0.001$ for each area, Bonferroni-adjusted for 35 multiple comparisons). Table 1 shows the PC/decade volume reduction for each cortical area. Examples from the two areas with the lowest (frontal pole) and highest reduction rates (rostral anterior cingulate) are shown in Fig. 1, *A* and *B*, respectively. The overall frequency distribution of the mean PC/decade volume reduction in the 35 areas is shown in Fig. 2*A*, and the rates for individual areas in cortical lobes are shown in Fig. 2*B*.

Effect of Sex

With respect to differences between sexes, we found the following. First, all areas showed a statistically significant reduction in volume with age for both men and women ($P < 0.001$ for each area, Bonferroni-corrected). Second, the percent volume reduction rate with age was higher in men than in women for 30/35 (85.7%) areas (Fig. 3*A*), a highly statistically significant proportion ($P < 0.001$, Wilson test against the null hypothesis of 50%). Third, the overall rate of volume loss with age was significantly higher in men than in women ($P < 0.001$, paired t test, n = 35 areas). Finally, with respect to cortical lobes, a higher volume reduction rate was observed in men than in women (Fig. 3*B*), a difference that reached statistical significance for the frontal and cingulate lobes (P = 0.034 and 0.004, respectively; paired t test).

DISCUSSION

The results of this study confirm previous findings on brain volume reduction with age (1–8) and its modulation

Table 1. *Percent reduction of volume with age per decade in individual cortical areas*

	Area	Lobe	% Volume Reduction/Decade			
			Men	Women	Mean	Deviation from Grand Mean
1	Caudal middle frontal gyrus	Frontal	−6.241	−6.034	−6.138	−0.860
2	Frontal pole	Frontal	−3.782	−2.767	−3.275	2.004
3	Inferior frontal gyrus pars opercularis	Frontal	−5.429	−4.781	−5.105	0.173
4	Inferior frontal gyrus pars orbitalis	Frontal	−5.473	−5.372	−5.423	−0.145
5	Inferior frontal gyrus pars triangularis	Frontal	−5.826	−5.031	−5.429	−0.151
6	Lateral orbital frontal cortex	Frontal	−4.879	−4.518	−4.699	0.580
7	Medial orbital frontal cortex	Frontal	−3.413	−2.767	−3.090	2.188
8	Paracentral lobule	Parietal	−5.117	−4.868	−4.993	0.286
9	Precentral gyrus	Frontal	−5.349	−5.075	−5.212	0.066
10	Rostral middle frontal gyrus	Frontal	−6.088	−6.834	−6.461	−1.183
11	Superior frontal gyrus	Frontal	−5.904	−5.688	−5.796	−0.518
12	Cuneus cortex	Parietal	−5.416	−4.528	−4.972	0.306
13	Inferior parietal cortex	Parietal	−5.834	−5.885	−5.860	−0.582
14	Insula	Parietal	−4.437	−4.257	−4.347	0.931
15	Postcentral gyrus	Parietal	−5.234	−5.231	−5.233	0.045
16	Superior parietal cortex	Parietal	−5.294	−5.548	−5.421	−0.143
17	Supramarginal gyrus	Parietal	−6.131	−6.040	−6.086	−0.808
18	Banks superior temporal sulcus	Temporal	−5.712	−5.632	−5.672	−0.394
19	Entorhinal cortex	Temporal	−3.660	−4.848	−4.254	1.024
20	Fusiform gyrus	Temporal	−5.355	−5.295	−5.325	−0.047
21	Hippocampus	Temporal	−4.623	−4.091	−4.357	0.921
22	Inferior temporal gyrus	Temporal	−6.458	−6.686	−6.572	−1.294
23	Middle temporal gyrus	Temporal	−6.640	−6.217	−6.429	−1.151
24	Parahippocampal gyrus	Temporal	−4.208	−3.950	−4.079	1.199
25	Superior temporal gyrus	Temporal	−5.846	−5.347	−5.597	−0.319
26	Temporal pole	Temporal	−3.735	−3.293	−3.514	1.764
27	Transverse temporal cortex	Temporal	−5.507	−4.724	−5.116	0.163
28	Lateral occipital cortex	Occipital	−5.750	−5.192	−5.471	−0.193
29	Lingual gyrus	Occipital	−5.187	−4.906	−5.047	0.232
30	Pericalcarine cortex	Occipital	−5.561	−4.226	−4.894	0.385
31	Precuneus cortex	Occipital	−6.178	−5.668	−5.923	−0.645
32	Caudal anterior cingulate cortex	Cingulate	−6.362	−5.563	−5.963	−0.685
33	Isthmus cingulate cortex	Cingulate	−6.118	−5.530	−5.824	−0.546
34	Posterior cingulate cortex	Cingulate	−6.081	−5.625	−5.853	−0.575
35	Rostral anterior cingulate cortex	Cingulate	−7.588	−7.027	−7.308	−2.030

Grand mean = −5.278.

by sex (16). The rate of volume reduction differed for different areas (Table 1), as has been reported previously (1–3, 7). Moreover, the rate of volume reduction was consistently greater in men with respect to both the number of areas affected and the magnitude of the reduction rate. Interestingly, the highest differential between men and women was observed in the cingulate cortex.

The reasons for the variation of the rate of volume reduction with age among different areas are unclear. Since brain gray matter atrophy is prevented by the presence of Human Leukocyte Antigen (HLA) DRB1*13:02 allele (17), it has been hypothesized that an overall factor involved in brain atrophy is direct damage and associated neuroinflammation induced by persistent foreign antigens that are not eliminated from

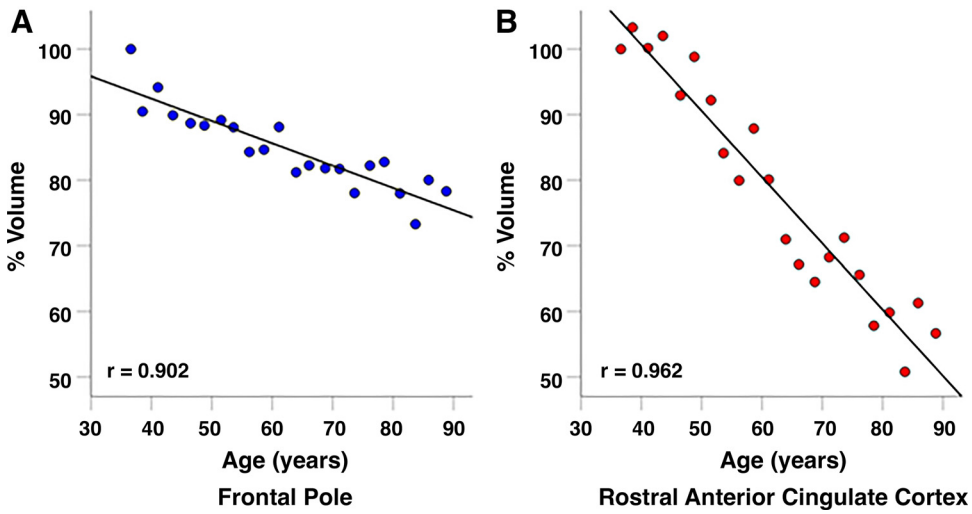

Figure 1. *A*: percent reduction of volume per decade for frontal pole. Data points are for 2.5 yr age bins ($r = -0.902$, $P < 0.001$, $n = 22$ bins). *B*: percent reduction of volume per decade for rostral anterior cingulate cortex. Data points are for 2.5-yr age bins ($r = -0.962$, $P < 0.001$, $n = 22$ bins).

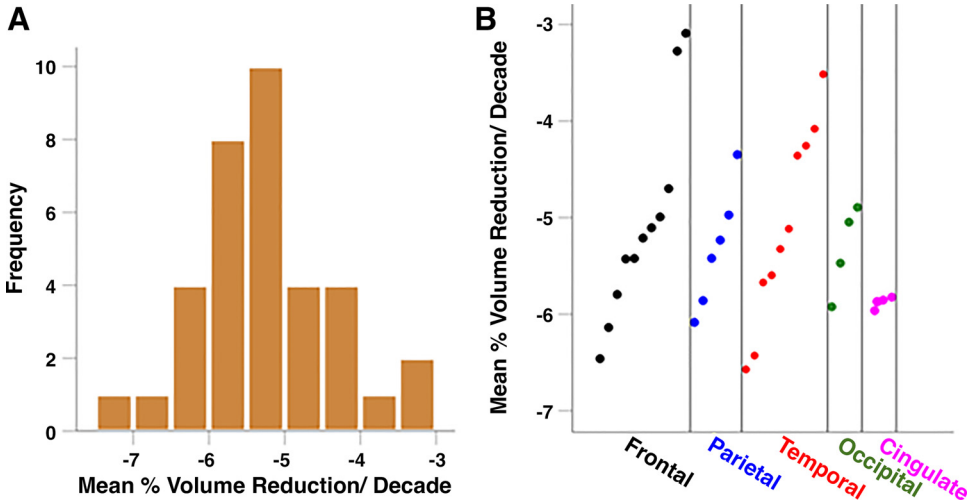

Figure 2. *A*: frequency distribution of the percent volume reduction (n = 35 areas). *B*: percent volume reduction for individual areas is plotted ranked separately for each lobe.

the body in the absence of matching HLA molecules (17). The same mechanism has been postulated to underlie the prevention of brain atrophy in Gulf War Illness (18) by the presence of DRB1*13:02 and other protective alleles (19, 20). In the context of this hypothesis positing a detrimental role of persistent antigens/neuroinflammation in brain atrophy, the differential rates of reduction of gray matter with age would be attributed to a differential vulnerability of individual brain regions resulting from differential exposure to persistent antigens (e.g., latent viruses), differential availability of local defense mechanisms (e.g., native and adaptive immunity), and differential local inflammatory response, to name but a few relevant factors. The extent of involvement of such factors would differ among brain regions, depending on, but not limited to, the anatomical location of the region (e.g., proximity to blood brain barrier), availability of adequate local blood supply, the local presence of neuromodulators [e.g., acetylcholine, a known vasodilator (21, 22)] and immunomodulators [e.g., intercellular adhesion molecule 5 (23, 24)], the presence of apolipoprotein E molecules (25), etc. The specific role of those and other factors in contributing to local vulnerability/protection against neuronal loss remains to be determined.

The highest rate of volume reduction with age was observed for the rostral anterior cingulate cortex (rACC). This area is a key node in emotional-cognitive processing (26, 27) and has been consistently implicated in depression (28). Interestingly, its volume has been found to be a good predictor of therapeutic intervention by ketamine (29), transcranial magnetic stimulation (30), and internet-based cognitive therapy (31), such that larger rACC pretreatment volumes are associated with a more favorable response to subsequent treatment. Moreover, depressive symptoms and diagnoses have been associated with reduced thickness of rACC (32). With respect to depression and aging, it is well established that the prevalence of depression increases with age (33, 34), and for older people depression has been

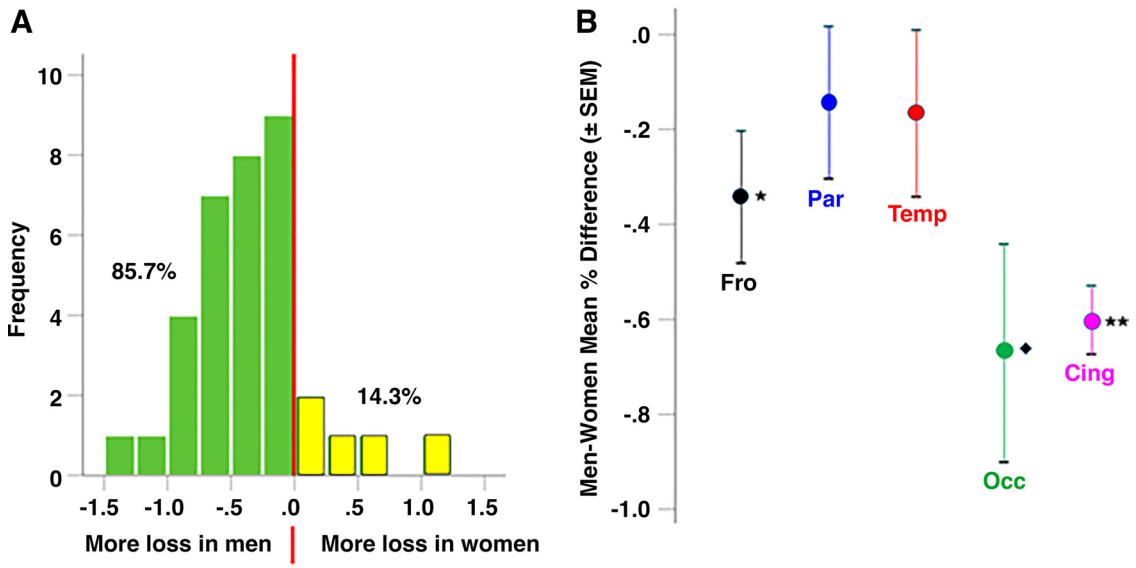

Figure 3. *A*: frequency distribution of the difference in percent volume reduction per decade between men and women (% reduction in men − % reduction in women). n = 35 areas. *B:* means (±SE) difference in percent reduction of volume per decade between men and women (% Men − % Women) in the five cortical lobes. Cing, cingulate; Fro, frontal; M, men; Occ, occipital; Par, parietal; Temp, temporal; W, women. *P = 0.034; **P = 0.004; ◆P = 0.061 (see text for details).

recognized as a clinical entity requiring prevention and treatment (35). The increase of depression with age has been attributed to the cumulative effect of several factors (33, 34), including physical factors (decreased mobility, appearance/presence of various diseases, etc.) and social circumstances (family support issues, reduced socialization, loneliness, etc.). Such factors seem to play a more important role in women and have been hypothesized to contribute to the higher prevalence of old-age depression in women than men (34). The results of our study suggest that the substantial decrease with age of the volume of rACC could be an underlying biological substrate mediating the effects of the various factors aforementioned.

DATA AVAILABILITY

Data are publicly available from the websites mentioned in the Materials and Methods section.

GRANTS

Partial funding for this study was provided by the University of Minnesota (the Kunin Chair in Women's Healthy Brain Aging, the Brain and Genomics Fund, the McKnight Presidential Chair in Cognitive Neuroscience, the American Legion Brain Sciences Chair), and the U.S. Department of Veterans Affairs. Research reported in this publication was supported by the National Institute On Aging of the National Institutes of Health under Award Number U01AG052564 and by funds provided by the McDonnell Center for Systems Neuroscience at Washington University in St. Louis.

DISCLAIMERS

The sponsors had no role in the current study design, analysis or interpretation, or in the writing of this paper. The contents do not represent the views of the U.S. Department of Veterans Affairs or the United States Government. The content is solely the responsibility of the authors and does not necessarily represent the official views of the National Institutes of Health.

DISCLOSURES

No conflicts of interest, financial or otherwise, are declared by the authors.

AUTHOR CONTRIBUTIONS

P.C. and A.P.G. analyzed data; P.C. and A.P.G. interpreted results of experiments; A.P.G. prepared figures; P.C. and A.P.G. drafted manuscript; P.C. and A.P.G. edited and revised manuscript; P.C. and A.P.G. approved final version of manuscript.

REFERENCES

1. **Raz N**, **Ghisletta P**, **Rodrigue KM**, **Kennedy KM**, **Lindenberger U.** Trajectories of brain aging in middle-aged and older adults: regional and individual differences. *NeuroImage* 51: 501–511, 2010. doi:10.1016/j.neuroimage.2010.03.020.
2. **Lemaitre H**, **Goldman AL**, **Sambataro F**, **Verchinski BA**, **Meyer-Lindenberg A**, **Weinberger DR**, **Mattay VS.** Normal age-related brain morphometric changes: nonuniformity across cortical thickness, surface area and gray matter volume? *Neurobiol Aging* 3: 617e.1-9, 2012. doi:10.1016/j.neurobiolaging.2010.07.013.
3. **Walhovd KB**, **Westlye LT**, **Amlien I**, **Espeseth T**, **Reinvang I**, **Raz N**, **Agartz I**, **Salat DH**, **Greve DN**, **Fischl B**, **Dale AM**, **Fjell AM.** Consistent neuroanatomical age-related volume differences across multiple samples. *Neurobiol Aging* 32: 916–932, 2012. doi:10.1016/j.neurobiolaging.2009.05.013.
4. **Jiang J**, **Sachdev P**, **Lipnicki DM**, **Zhang H**, **Liu T**, **Zhu W**, **Suo C**, **Zhuang L**, **Crawford J**, **Reppermund S**, **Trollor J**, **Brodaty H**, **Wen W.** A longitudinal study of brain atrophy over two years in community-dwelling older individuals. *NeuroImage* 86: 203–211, 2014. doi:10.1016/j.neuroimage.2013.08.022.
5. **Raz N**, **Rodrigue KM.** Differential aging of the brain: Patterns, cognitive correlates and modifiers. *Neurosci Biobehav Rev* 30: 730–748, 2006. doi:10.1016/j.neubiorev.2006.07.001.
6. **Goodro M**, **Sameti M**, **Patenaude B**, **Fein G.** Age effect on subcortical structures in healthy adults. *Psychiatry Res* 203: 38–45, 2012. doi:10.1016/j.pscychresns.2011.09.014.
7. **Fjell AM**, **Westlye LT**, **Grydeland H**, **Amlien I**, **Espeseth T**, **Reinvang I**, **Raz N**, **Holland D**, **Dale AM**, **Walhovd KB**; **Alzheimer Disease Neuroimaging Initiative.** Critical ages in the life course of the adult brain: nonlinear subcortical aging. *Neurobiol Aging* 34: 2239–2247, 2013. doi:10.1016/j.neurobiolaging.2013.04.006.
8. **Dima D**, **Modabbernia A**, **Papachristou E**, **Doucet GE**, **Agartz I**, **Aghajani M et al.** Subcortical volumes across the lifespan: data from 18,605 healthy individuals aged 3–90 years. *Hum Brain Mapp* 43: 452–469, 2022. doi:10.1002/hbm.25320.
9. **Bookheimer SY**, **Salat DH**, **Terpstra M**, **Ances BM**, **Barch DM**, **Buckner RL**, **Burgess GC**, **Curtiss SW**, **Diaz-Santos M**, **Elam JS**, **Fischl B**, **Greve DN**, **Hagy HA**, **Harms MP**, **Hatch OM**, **Hedden T**, **Hodge C**, **Japardi KC**, **Kuhn TP**, **Ly TK**, **Smith SM**, **Somerville LH**, **Uğurbil K**, **van der Kouwe A**, **Van Essen D**, **Woods RP**, **Yacoub E.** The LifespanHuman Connectome Project in aging: an overview. *NeuroImage* 185: 335–348, 2019. doi:10.1016/j.neuroimage.2018.10.009.
10. **Harms MP**, **Somerville LH**, **Ances BM**, **Andersson J**, **Barch DM**, **Bastiani M et al.** Extending the Human Connectome Project across ages: Imaging protocols for the Lifespan Development and Aging projects. *NeuroImage* 183: 972–984, 2018. doi:10.1016/j.neuroimage.2018.09.060.
11. **Glasser MF**, **Sotiropoulos SN**, **Wilson JA**, **Coalson TS**, **Fischl B**, **Andersson JL**, **Xu J**, **Jbabdi S**, **Webster M**, **Polimeni JR**, **Van Essen DC**, **Jenkinson M**; **WU-Minn HCP Consortium.** The minimal preprocessing pipelines for the Human Connectome Project. *NeuroImage* 80: 105–124, 2013. doi:10.1016/j.neuroimage.2013.04.127.
12. **Dale AM**, **Fischl B**, **Sereno MI.** Cortical surface-based analysis. I. Segmentation and surface reconstruction. *NeuroImage* 9: 179–194, 1999. doi:10.1006/nimg.1998.0395.
13. **Desikan RS**, **Ségonne F**, **Fischl B**, **Quinn BT**, **Dickerson BC**, **Blacker D**, **Buckner RL**, **Dale AM**, **Maguire RP**, **Hyman BT**, **Albert MS**, **Killiany RJ.** An automated labeling system for subdividing the human cerebral cortex on MRI scans into gyral based regions of interest. *NeuroImage* 31: 968–980, 2006. doi:10.1016/j.neuroimage.2006.01.021.
14. **Zar JH.** *Biostatistical Analysis* (5th ed.). London, UK: Pearson, 2009.
15. **Wilson EB.** Probable inference, the law of succession, and statistical inference. *J Am Stat Assoc* 22: 209–212, 1927. doi:10.1080/01621459.1927.10502953.
16. **Lemaître H**, **Crivello F**, **Grassiot B**, **Alpérovitch A**, **Tzourio C**, **Mazoyer B.** Age- and sex-related effects on the neuroanatomy of healthy elderly. *NeuroImage* 26: 900–911, 2005. doi:10.1016/j.neuroimage.2005.02.042.
17. **James LM**, **Christova P**, **Lewis SM**, **Engdahl BE**, **Georgopoulos A**, **Georgopoulos AP.** Protective effect of human leukocyte antigen (HLA) allele DRB1*13:02 on age-related brain gray matter volume reduction in healthy women. *EBioMedicine* 29: 31–37, 2018. doi:10.1016/j.ebiom.2018.02.005.
18. **Christova P**, **James LM**, **Engdahl BE**, **Lewis SM**, **Carpenter AF**, **Georgopoulos AP.** Subcortical brain atrophy in Gulf War illness. *Exp Brain Res* 235: 2777–2786, 2017. doi:10.1007/s00221-017-5010-8.
19. **James LM**, **Christova P**, **Engdahl BE**, **Lewis SM**, **Carpenter AF**, **Georgopoulos AP.** Human leukocyte antigen (HLA) and Gulf War Illness (GWI): HLA-DRB1*13:02 spares subcortical atrophy in Gulf War veterans. *Ebiomedicine* 26: 126–131, 2017. doi:10.1016/j.ebiom.
20. **Christova P**, **James LM**, **Carpenter AF**, **Lewis SM**, **Engdahl BE**, **Georgopoulos AP.** Human leukocyte antigen (HLA) alleles prevent metabolically-induced inflammation and cerebrocortical thinning in gulf war illness. *J Neurol Neuromed* 5: 16–27, 2020. doi:10.29245/2572.942X/2020/3.1273.
21. **Heistad DD**, **Marcus ML**, **Said SI**, **Gross PM.** Effect of acetylcholine and vasoactive intestinal peptide on cerebral blood flow. *Am J*

Physiol Heart Circ Physiol 239: H73–H80, 1980. doi:10.1152/ajpheart.1980.239.1.H73.
22. **Scremin OU**, **Jenden DJ.** Cholinergic control of cerebral blood flow in stroke, trauma and aging. *Life Sci* 58: 2011–2018, 1996. doi:10.1016/0024-3205(96)00192-0.
23. **Tian L**, **Lappalainen J**, **Autero M**, **Hänninen S**, **Rauvala H**, **Gahmberg CG.** Shedded neuronal ICAM-5 suppresses T-cell activation. *Blood* 111: 3615–3625, 2008. doi:10.1182/blood-2007-09-111179.
24. **Tian L**, **Rauvala H**, **Gahmberg CG.** Neuronal regulation of immune responses in the central nervous system. *Trends Immunol* 30: 91–99, 2009. doi:10.1016/j.it.2008.11.002.
25. **Huang Y**, **Mahley RW.** Apolipoprotein E: structure and function in lipid metabolism, neurobiology, and Alzheimer's diseases. *Neurobiol Dis* 72: 3–12, 2014. doi:10.1016/j.nbd.2014.08.025.
26. **Bissière S**, **Plachta N**, **Hoyer D**, **McAllister KH**, **Olpe HR**, **Grace AA**, **Cryan JF.** The rostral anterior cingulate cortex modulates the efficiency of amygdala-dependent fear learning. *Biol Psychiatry* 63: 821–831, 2008. doi:10.1016/j.biopsych.2007.10.022.
27. **Tang W**, **Jbabdi S**, **Zhu Z**, **Cottaar M**, **Grisot G**, **Lehman JF**, **Yendiki A**, **Haber SN.** A connectional hub in the rostral anterior cingulate cortex links areas of emotion and cognitive control. *Elife* 8: e43761, 2019. doi:10.7554/eLife.43761.
28. **Jin J**, **Delaparte L**, **Chen HW**, **DeLorenzo C**, **Perlman G**, **Klein DN**, **Mohanty A**, **Kotov R.** Structural connectivity between rostral anterior cingulate cortex and amygdala predicts first onset of depressive disorders in adolescence. *Biol Psychiatry Cogn Neurosci Neuroimaging* 7: 249–255, 2022. doi:10.1016/j.bpsc.2021.01.012.
29. **Herrera-Melendez A**, **Stippl A**, **Aust S**, **Scheidegger M**, **Seifritz E**, **Heuser-Collier I**, **Otte C**, **Bajbouj M**, **Grimm S**, **Gärtner M.** Gray matter volume of rostral anterior cingulate cortex predicts rapid antidepressant response to ketamine. *Eur Neuropsychopharmacol* 43: 63–70, 2021. doi:10.1016/j.euroneuro.2020.11.017.
30. **Boes AD**, **Uitermarkt BD**, **Albazron FM**, **Lan MJ**, **Liston C**, **Pascual-Leone A**, **Dubin MJ**, **Fox MD.** Rostral anterior cingulate cortex is a structural correlate of repetitive TMS treatment response in depression. *Brain Stimul* 11: 575–581, 2018. doi:10.1016/j.brs.2018.01.029.
31. **Webb CA**, **Olson EA**, **Killgore WDS**, **Pizzagalli DA**, **Rauch SL**, **Rosso IM.** Rostral anterior cingulate cortex morphology predicts treatment response to internet-based cognitive behavioral therapy for depression. *Biol Psychiatry Cogn Neurosci Neuroimaging* 3: 255–262, 2018. doi:10.1016/j.bpsc.2017.08.005.
32. **Binnewies J**, **Nawijn L**, **van Tol MJ**, **van der Wee NJA**, **Veltman DJ**, **Penninx BWJH.** Associations between depression, lifestyle and brain structure: a longitudinal MRI study. *NeuroImage* 231: 117834, 2021. doi:10.1016/j.neuroimage.2021.117834.
33. **Mirowsky J**, **Ross CE.** Age and depression. *J Health Soc Behav* 33: 187–205, 1992.
34. **Cheung ESL**, **Mui AC.** Gender variation and late-life depression: findings from a national survey in the USA. *Ageing Int* 8: 1–18, 2021. doi:10.1007/s12126-021-09471-5.
35. **Almeida OP.** Prevention of depression in older age. *Maturitas* 79: 136–141, 2014. doi:10.1016/j.maturitas.2014.03.005.